Iraqi Journal of Physics, 2018 *Vol.16, No.36, PP. 11-28*

DOI: 10.20723/ijp.16.36.11-28

The effect of gold nanoparticles on WO_3 thin film

Isam M. Ibrahim[1], Niran F. Abdul-Jabbar[2], Abeer H. Fezaa[2]

[1]Department of Physics, College of Science, University of Baghdad

[2]Department of Physics, College of Education, University of Tikrit

E-mail: dr.issamiq@gmail.com

Abstract

Chemical spray pyrolysis technique was used at substrate temperature 250 ˚C with annealing temperature at 400 ˚C (for 1hour) to deposition tungsten oxide thin film with different doping concentration of Au nanoparticle (0, 10, 20, 30 and 40)% wt. on glass substrate with thickness about 100 nm. The structural, optical properties were investigated. The X-ray diffraction shows that the films at substrate temperature (250 ˚C) was amorphous while at annealing temperature have a polycrystalline structure with the preferred orientation of (200), all the samples have a hexagonal structure for WO_3 and Au gold nanoparticles have a cubic structure. Atomic force microscopy (AFM) was used to characterize the morphology of the films. The optical properties of the films were studied using UV-Vis spectrophotometer within the wavelength in the range (300-1100) nm. The optical energy gap of the films was (2.80) eV for WO_3 and it decreased at annealing temperature (400 ˚C) equal to (2.65) eV. And finally the optical constants such as refractive index, real and imaginary dielectrics, absorption coefficient, absorption, transmission, and extinction coefficient were investigated.

Key words

Tungsten oxide, Au, annealing temp., chemical spray pyrolysis.

Article info.

Received: May. 2017
Accepted: Jul. 2017
Published: Mar. 2018

تاثير الجزيئات النانوية للذهب على الاغشية الرقيقة للتنكستن

عصام محمد ابرهيم[1]، نيران فاضل عبد الجبار[2]، عبير حاتم فزع[2]

[1]قسم الفيزياء، كلية العلوم، جامعة بغداد

[2]قسم الفيزياء، كلية التربية، جامعة تكريت

الخلاصة

أستخدامت طريقة التحليل الكيميائي الحراري عند حرارة 250 ˚C و لدنت هذه الاغشية لمدة ساعة بحرارة 400 ˚C، لترسيب اغشية رقيقة من اوكسيد التنكستن بتراكيز تطعيم مختلفة من جزيئات الذهب النانوية (0، 10، 20، 30 و 40) wt. %، على قواعد زجاجية وبسمك حوالي 100 nm، أجريت الفحوصات التركيبية والبصرية، بينت من الخصائص التركيبية للاغشية المحضرة على الارضيات الزجاجية باستخدام حيود الاشعة السينية XRD انها تمتلك طور غير متبلور عند حرارة 250 ˚C، وتمتلك تركيب متعدد البلورات وبالطور السداسي لاوكسيد التنكستن وبالاتجاه المفضل (200) وان اغشية WO_3 المشوبة بالذهب لها تركيب في الطور مكعب عند حرارة تلدين 400 ˚C أستخدم المجهر القوة الذرية لتعيين طبيعة السطح كما درست الخصائص البصرية باستخدام مطياف الاشعة فوق البنفسجية والاشعة المرئية مع طول موجي يتراوح بين 300- nm (1100). وكانت فجوة الطاقة البصرية لاغشية التنكستن eV (2.80) تناقصت مع حرارة التلدين الى eV (2.65). وتم حساب الثوابت البصريه الاخرى مثل معامل الانكسار، النفاذية، الامتصاصية، معامل الخمود وثابت العزل الحقيقي والخيالي، ومعامل الامتصاص للاغشيه المحضره.

Introduction

Over the last few years, interest in tungsten trioxide (WO_3) has increased rapidly and significantly due to the materials potential applications in photo voltaic and photo catalytic processes [1]. WO_3 is a cheap material, with excellent chemical stability, nontoxicity, good mechanical properties and is one of the most efficient semiconductor photo catalyst for extensive environmental applications because of its strong oxidizing power, high photochemical corrosive resistance and cost effectiveness[2, 3]. There are many techniques to synthesize WO_3 thin films, including sol–gel, sputtering, anodic oxidation, pulsed laser deposition (PLD), electron-beam evaporation and spray pyrolysis [4]. Easy and fast in preparing thin film with requisite specifications because of the existence of the chemical materials and the film formed immediately after the chemical reaction takes place on the hot substrate The film which is prepared by the spray technique has high stability with time in its physical properties [5]. Noble metal nanoparticles such as Au NPs have been a source of great interest due to their novel electrical, optical, physical, chemical and magnetic properties [6, 7]. Among nanomaterial's, gold (Au) NPs are especially attractive as they exhibit vibrant optical absorbance, high dispersibility in aqueous medium, chemical inertness, and biocompatibility [8, 9] to improve characteristics of metal oxide films can be Gained by adding small amounts of dopants into the pure MOS materials. Intentional impurities, or dopants, used to control the behavior of materials lies at the heart of many technologies. Dopants can influence semiconductor Nanocrystals, crystallites a few nanometers in scale with unusual and size specific optical and electronic behavior [10]. In this research the essential aim of work to prepare a pure WO_3 thin films and doped Au by using chemical spray pyrolysis method at different concentration (0, 10, 20, 30 and 40) %wt. and study the structural and optical properties of these prepared samples.

Experimental procedure

Preparation solution

The solution was prepared by mixed HCl and H_2O_2 to get WCl_6 .The molar concentration of the solution must be equal to 0.05 mol/ litter. To prepare the solution of 0.05 molar concentrations from these two materials, few grams weight are needed from each of them, heated 90 ml of distilled water, according to the following equation:

Weight of the material (g) =Volume (ml) × Molecular concentration (mol/l) ×Molecular weight (g/mol) (1)

According to Eq. (1), the weight which is required from tungsten material can be calculated as following:

The weight of WO_3= (231.84×0.05 ×100) / 1000= 1.1592g.

where the molecular weight of the WO_3= 231.84 g / mol

A digital balance type "Mettler AE-160" with an accuracy of 10^{-4} g is used for weighting the needed material.

Finally, the weight material heated in (100 ml) of distilled water to get the wanted solution. Then, it was putting on the magnetic stirrer for 15 minutes to be sure that the mixture solutions are well mixed. After then the solution was ready for using.

Thin film preparation of WO_3

Chemical spray pyrolysis method, thin films were prepared by spraying the solution on a hot glass substrate at a temperature about (250 ˚C), and the film will be formed by the chemical

reaction of the prepared solution on the hot substrate. To get the finally WO_3 thin film according to the following chemical equation [11]

$$2WCl_6 + 3O_2 \xrightarrow{\Delta} 2WO_3 + 6\,Cl_2 \qquad (2)$$

It is necessary to leave the glass substrate on the electrical heater for one hour at least after finishing the operation of spraying to complete its oxidation and crystalline growth process. In the spray system, compressed and purified air was used as the carrier gas with a 3 kg / cm^2 pressure and the spraying solution 0.05 M concentration, the distance between the spray nozzle and the substrate was fixed at 22 cm the deposition rate is ~5 min, then the substrates can be raised.

Preparation of Au nano solution

Nanoparticles gold solution was prepared by (Nd-YAG Laser) type (HUAFEI) at a wavelength (1064 nm) and frequency of pulses (6 Hz), using removal by leaser inside solution. Putting small pieces of high gold purity (99.99 %) in glass container contains (2 ml) of distilled water. The distance between the target and laser beam was (12 cm), the energy required for preparation was (500 mJ) and the number of pulses (200 pulse) the time for preparation was (6 min). Many tests were used to examine the produced thin film such as XRD, UV- Vis., and AFM.

Results and discussion

1-X-ray diffraction

Fig.1 shows XRD patterns of WO_3 thin films with doping by gold nanoparticles as prepared at 250 ˚C were amorphous structure this results agree with Myong and et al. [12] and with Ayat and et al. [13], the addition of Au gold nanoparticles into WO_3 did not improve the structure of WO_3 up to Au concentration of 40 %, as evidenced from the absence of XRD peaks, however, at higher Au concentration (40 %) there was still no improvement in the structure of WO_3, Fig. 2 shows annealed films at 400˚C, many small and high peaks was showed in pure film are belongs to WO_3 this obtain that the film is a polycrystalline and the preferential orientation of the film was a long the plan (200) at diffraction angle of $2\theta = 28.1900^{\circ}$ which in agreement with [12, 14]. When the Au was added at ratio 10%, new one peak (200) was appeared belongs to Au at $2\theta = 44.4118^{\circ}$. An additional peak was appear (111) at $2\theta = 37.8210^{\circ}$ is also belongs to Au was showed in the ratio 20 %. In the ratios 30 % and 40 % the intensity of peaks of Au becomes to increases and the peak's intensity of WO_3 gradually began to decrease ,all the samples have a hexagonal structure for WO_3 according to International Centre for Diffraction (card No.96-100-4058), and which is doped gold nanoparticles have a cubic structure according to the International Centre for Diffraction (96-901-2431), in the randomly there are defects and levels of the tail and at annealing are improving the composition of the material and rearrangement, which led to conversion to multiple crystallization its' mean removing some defects and gaps remained local levels and therefore the gap is less more than before. The crystallite size decreases by increasing the deflection, this is explained by the large diameter of the ion of the defect will be interface, which leads to the decrease in crystallite size and thus an increase of (2θ), the crystallite size is inversely propotional to the (FWHM) this is agree with [15-18], the average crystallite size was equal to (9.24) nm it was estimated with Debye – scherrer formula for the (200) reflection follow [19]:

$$D = \frac{0.94\,\lambda}{\beta\,COS\,\theta} \quad (3)$$

where λ is the wavelength of XRD photons which equal to 0.154 nm, β is the full width at half maximum (FWHM) and θ is the Brage diffraction angle in degrees. Eq. (3), where the relation between the crystallite size and FWHM is reverse. Decreasing in the crystallite size after doping is evidence on the improvement of the nanocrystal, which indicates that the deposited atoms of these films going towards nanostructure. There was a decrease in the D value when WO_3 films doped with Au dopant which indicate to nanoparticales formed which it was resulting from the doping process.

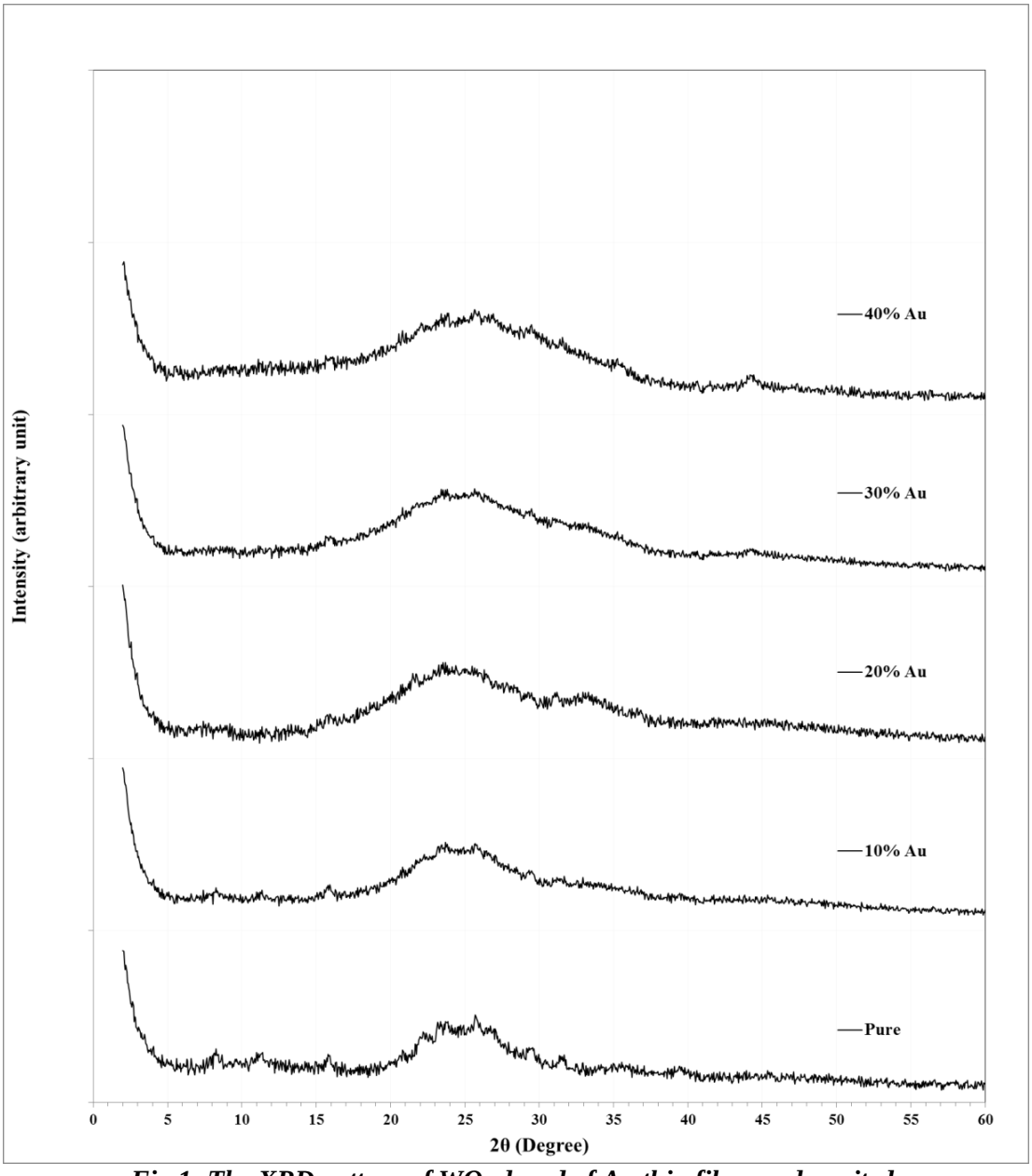

Fig.1: The XRD pattern of WO_3 doped of Au thin films as deposited.

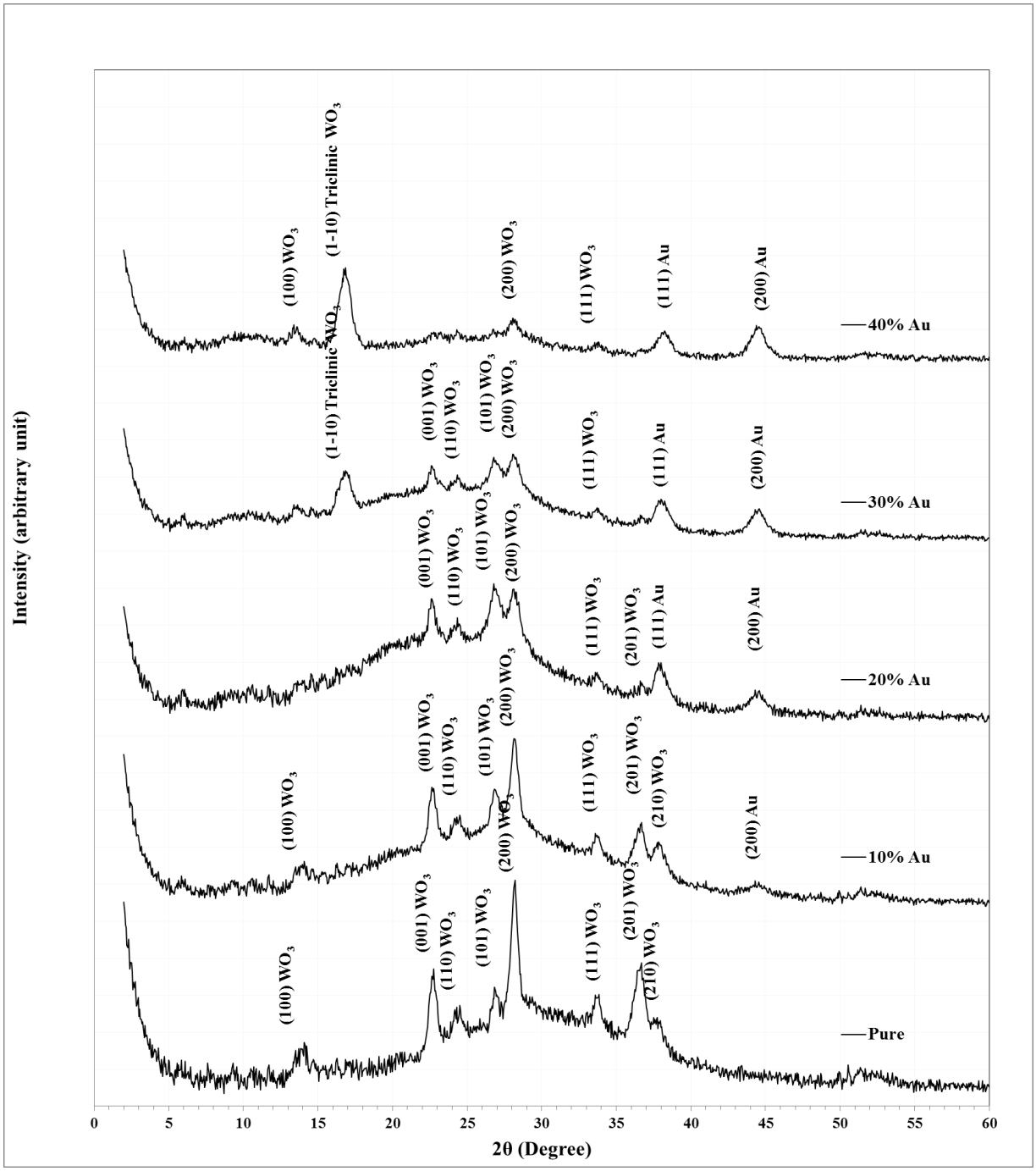

Fig. 2: The XRD pattern of WO_3 and doped of Au thin films with annealing temperature at T_a = 400 ˚C.

Table 1: Structural parameters vis. inter-planar spacing, crystalline size for pure WO_3 and Au thin films at T_a=400 ˚C.

Au%	2θ (Deg.)	FWHM (Deg.)	d_{hkl} Exp.(Å)	G.S (nm)	d_{hkl} Std.(Å)	Phase	hkl	card No.
Pure	13.9700	0.6988	6.3342	11.5	6.3203	Hex. WO_3	(100)	96-100-4058
	22.7100	0.5430	3.9124	14.9	3.8990	Hex. WO_3	(001)	96-100-4058
	24.3300	0.7431	3.6554	10.9	3.6490	Hex. WO_3	(110)	96-100-4058
	26.8800	0.4350	3.3142	18.8	3.3184	Hex. WO_3	(101)	96-100-4058
	28.1900	0.5320	3.1631	15.4	3.1601	Hex. WO_3	(200)	96-100-4058
	33.7400	0.6200	2.6544	13.4	2.6642	Hex. WO_3	(111)	96-100-4058
	36.5500	0.8325	2.4565	10.0	2.4550	Hex. WO_3	(201)	96-100-4058
	37.8000	0.7658	2.3781	11.0	2.3888	Hex. WO_3	(210)	96-100-4058
10	13.7500	0.9559	6.4351	8.4	6.3203	Hex. WO_3	(100)	96-100-4058
	22.6471	0.6618	3.9231	12.2	3.8990	Hex. WO_3	(001)	96-100-4058
	24.3382	0.6618	3.6542	12.3	3.6490	Hex. WO_3	(110)	96-100-4058
	26.8382	0.8088	3.3192	10.1	3.3184	Hex. WO_3	(101)	96-100-4058
	28.1618	0.7353	3.1662	11.1	3.1601	Hex. WO_3	(200)	96-100-4058
	33.6029	0.5882	2.6649	14.1	2.6642	Hex. WO_3	(111)	96-100-4058
	36.6912	0.8089	2.4474	10.3	2.4550	Hex. WO_3	(201)	96-100-4058
	37.7941	0.8089	2.3784	10.4	2.3888	Hex. WO_3	(210)	96-100-4058
	44.4118	1.1120	2.0382	7.7	2.0352	Cub. Au	(200)	96-901-2431
20	22.6420	0.5220	3.9240	15.5	3.8990	Hex. WO_3	(001)	96-100-4058
	24.3210	0.7220	3.6568	11.3	3.6490	Hex. WO_3	(110)	96-100-4058
	26.8754	0.9150	3.3147	8.9	3.3184	Hex. WO_3	(101)	96-100-4058
	28.1865	0.9700	3.1634	8.4	3.1601	Hex. WO_3	(200)	96-100-4058
	33.7344	0.6210	2.6548	13.4	2.6642	Hex. WO_3	(111)	96-100-4058
	36.5521	0.8140	2.4563	10.3	2.4550	Hex. WO_3	(201)	96-100-4058
	37.8210	0.7540	2.3768	11.1	2.3500	Cub. Au	(111)	96-901-2431
	44.5300	1.1700	2.0330	7.3	2.0352	Cub. Au	(200)	96-901-2431
30	16.8382	1.1029	5.2612	7.3	5.2170	Trec. WO_3	(1-10)	96-101-0619
	22.6471	0.5883	3.9231	13.8	3.8990	Hex. WO_3	(001)	96-100-4058
	24.3382	0.6618	3.6542	12.3	3.6490	Hex. WO_3	(110)	96-100-4058
	26.7647	0.8823	3.3282	9.3	3.3184	Hex. WO_3	(101)	96-100-4058
	28.0882	0.8088	3.1743	10.1	3.1601	Hex. WO_3	(200)	96-100-4058
	33.6765	0.8088	2.6592	10.3	2.6642	Hex. WO_3	(111)	96-100-4058
	38.0147	1.2500	2.3651	6.7	2.3500	Cub. Au	(111)	96-901-2431
	44.5588	1.1029	2.0318	7.8	2.0352	Cub. Au	(200)	96-901-2431
40	13.5000	0.6540	6.5537	12.2	6.3203	Hex. WO_3	(100)	96-100-4058
	16.8000	0.8650	5.2730	9.3	5.2170	Trec. WO_3	(1-10)	96-101-0619
	28.1643	0.9700	3.1659	8.4	3.1601	Hex. WO_3	(200)	96-100-4058
	33.7344	0.6210	2.6548	13.4	2.6642	Hex. WO_3	(111)	96-100-4058
	38.3534	0.9150	2.3450	9.2	2.3500	Cub. Au	(111)	96-901-2431
	44.5213	1.0600	2.0334	8.1	2.0352	Cub. Au	(200)	96-901-2431

2- Atomic force microscopic

Three-dimensional AFM images and the chart of grain density distribution for WO_3:Au as shown in Fig. 3. AFM images were taken in order to further observe microstructure and confirm the XRD result. The average diameter, average roughness and root mean square (r.m.s) are deduced from AFM images. The finer morphology and roughness of the films can be clearly seen for WO_3 thin films

with different doping of Au (10, 20, 30 and 40) % wt. before annealing. The result observe doping with 10% of Au average diameter, roughness average and root mean square decreases while for doping percent 30%, the average diameter, roughness and root mean square decreases. Figs. 3 and 4 show the morphological properties of the prepared pure and doped films at temperature before and after annealing at 400 ˚C, respectively. A sponge-like structure was appearing and the film covered all the surface of the glass substrate. From Table 2, the average diameter of WO_3 film is 90.59 nm before annealing, when the Au was added, the average diameter is decrease. The roughness and the RMS are varies when the Au is added and the maximum value was at Au ratio 20 %. From XRD and AFM results concluded that the ratio of 20 % Au is the best between the other ratios (smallest crystalline size and highest roughness) it can be used in manufacturing different devices such as optoelectronic devices.

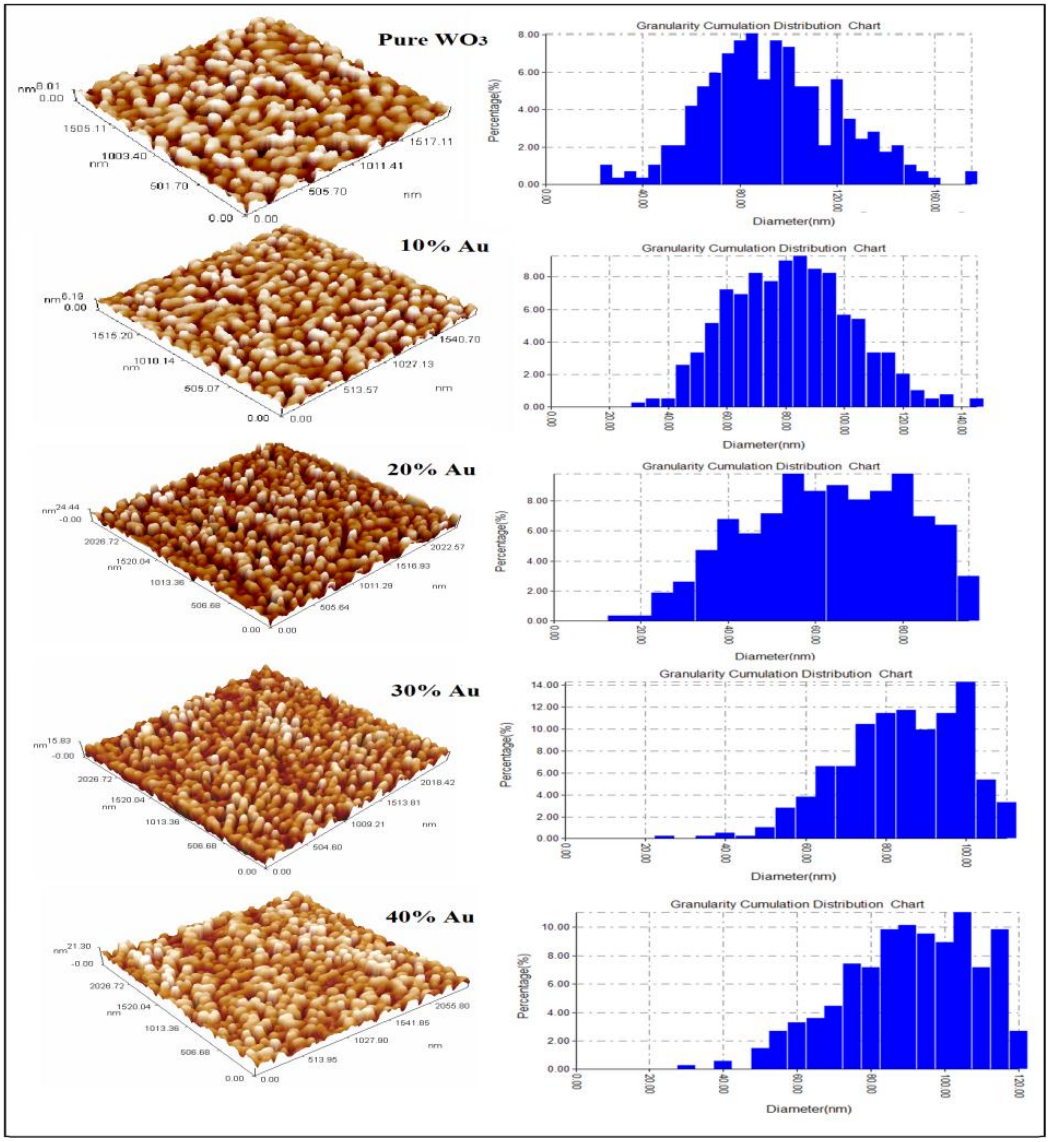

Fig. 3: AFM image and size distribution for pure WO_3 and doping with different ratio of Au thin films at room temperature 250 ˚C.

Table 2: Morphology parameters for pure WO_3 and doping with different ratio of Au thin films.

Au (%)	Ave. diameter(nm)	Roughness average(nm)	Root mean square(nm)
0	90.59	1.56	1.87
10	79.60	1.15	1.39
20	60.36	4.93	5.90
30	81.43	2.73	3.30
40	88.25	3.48	4.22

When the annealing temperature raised to 400 ˚C for pure WO_3 films and doped by Au, each of average diameter, roughness, and RMS was increase comparative with the film's properties before annealing it can be explained that the annealing and doping of Au improve the surface properties also the successive grain growth as result of the annealing at 400 ˚C [see Table 3]. The roughness of these films increases due to the existence of many hillocks, which are faceted and distributed randomly on the relatively smooth surface, so the increase of roughness can be explained by the grain growth and some structure densification of the deposition processes [20].

Table 3: Morphology parameters for WO_3 and doping with different ratio of Au thin films with annealing temperature at T_a=400 ˚C.

Au (%)	Ave. diameter (nm)	Roughness average (nm)	Root mean square (nm)
0	96.70	5.82	6.77
10	88.72	3.98	4.88
20	77.27	2.21	2.60
30	92.76	2.81	3.39
40	100.57	4.89	5.39

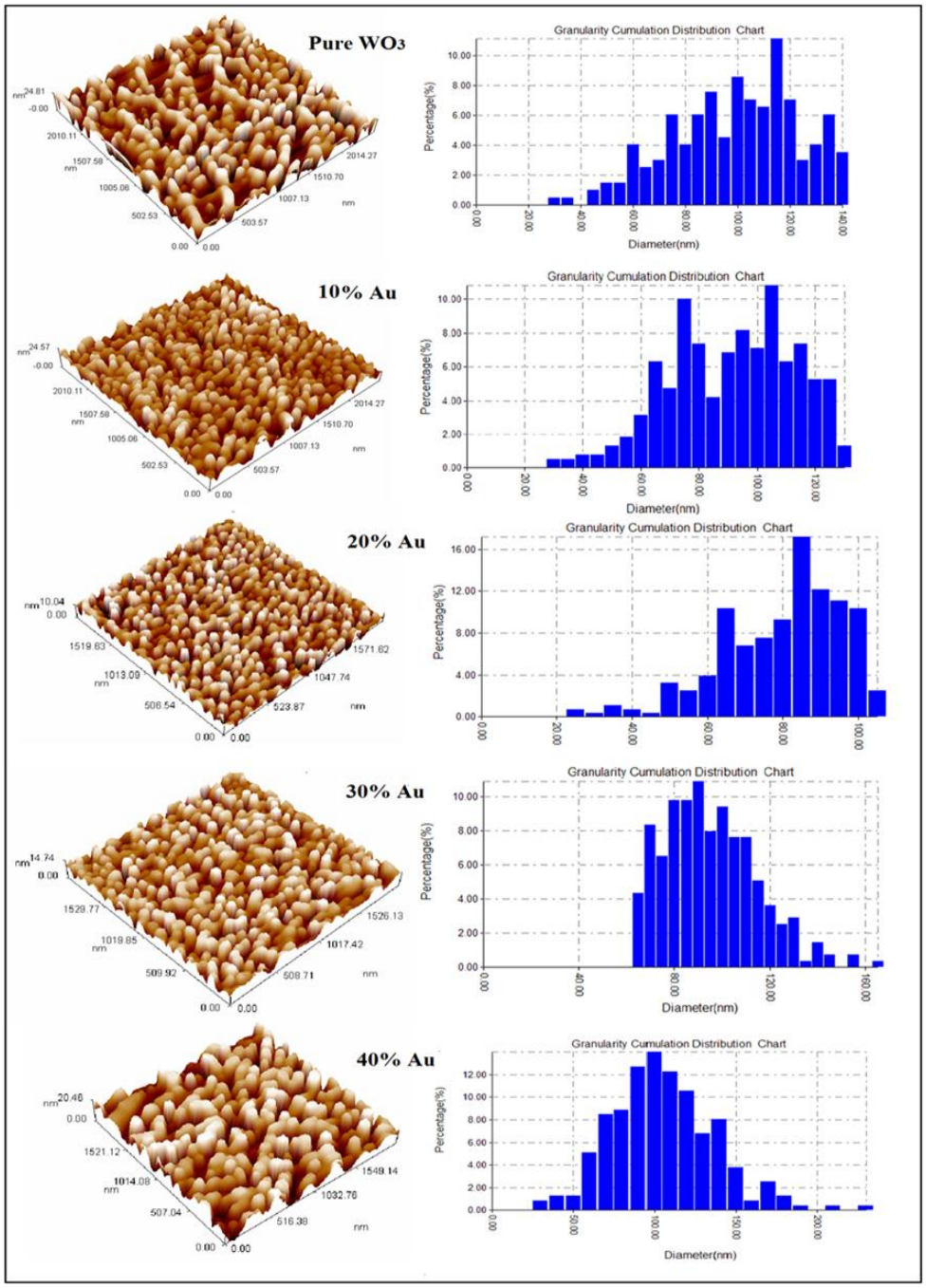

Fig. 4: AFM image and size distribution for WO_3 and doping with different ratio of Au thin films with annealing temperature at T_a=400 ˚C.

3- Optical properties

The optical properties of pure WO_3 thin film and doped with different concentrations of Au (0, 10, 20, 30 and 40)%wt. such transmission, absorption coefficient, Extinction coefficient, Refractive index, dielectric constant, and optical energy gap was measured before and after annealing at 400 ˚C.

3-1 The transmission spectrum

From transmission spectra illustrates in Figs. 5 and 6, before and after annealing at 400 ˚C the films showed high transmittance when the Au was added and increased from 3.89% for pure film to 34.34% for 30% Au ratio before annealing and increased from 1.92% for pure film to

22.09 % for 20 % Au ratio after annealing. In general the transmittance increase with increasing of doping ratio as a result of decreasing the absorbance and it was shown that the transmittance decreased for pure and doped films after annealing due to the enhancement of the absorption. The high transmittance of films throughout the UV-VIS regions makes it good material for optoelectronic devices.

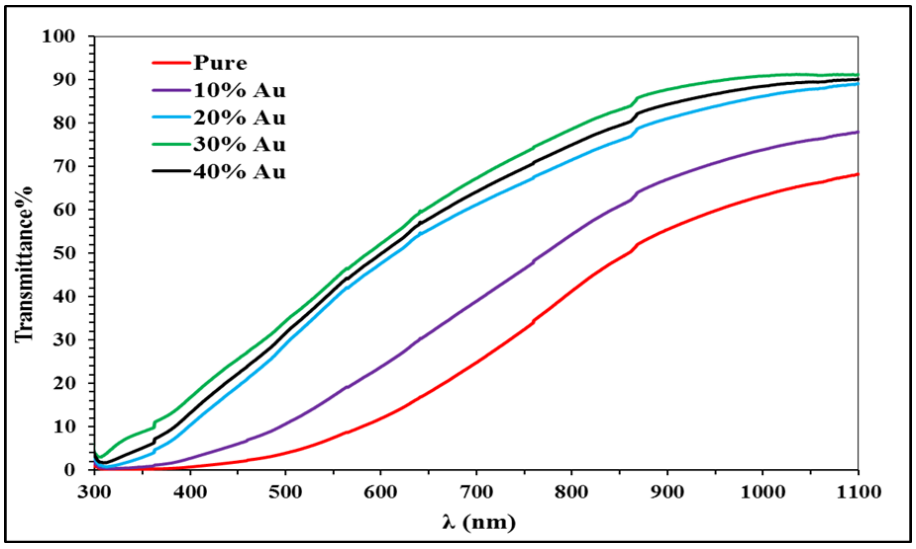

Fig. 5: The transmission spectrum for pureWO_3 and doped of Au (0, 10, 20, 30 and 40)% films as a function of wavelength.

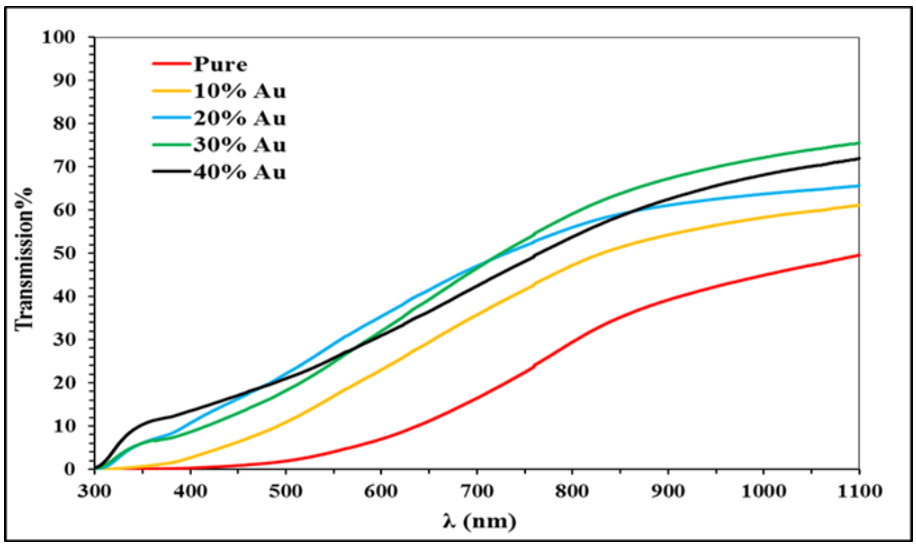

Fig. 6: The transmission spectrum for pureWO_3 and doped Au (0, 10, 20, 30 and 40)% films as a function of wavelength at T_a=400 ˚C.

3-2 Absorption coefficient

From Figs. 7 and 8 it can be noticed that the value of the absorption coefficient of thin films are of the order of (10^4) cm^{-1} which supports the direct band gap nature as well as, it can be seen that the absorption through WO_3 thin films is relatively high at below band gap region which indicating a high concentration of free carriers, the values of the absorption is attributed that the incoming photon have the sufficient energy to excite the electrons from the valence band to the conduction band, the absorption decreases when the wavelength

increasing and this decrease corresponds to the reduction in the photons energy. The absorbance coefficient also decreases with increasing of doping ratio (0, 10, 20, 30 and 40) %wt. Au. After annealing at 400˚C we can notice that the absorbance coefficient decreases due to the direct electronic transitions, α is the absorption coefficient, which is obtained near the absorption edge from the transmittance, T, using the equation [21, 22]:

$$\alpha = [1/t] \ln [T/(1-R)^2] \quad (4)$$

where T is the transmittance, R is the reflectance, and t is the film thickness.

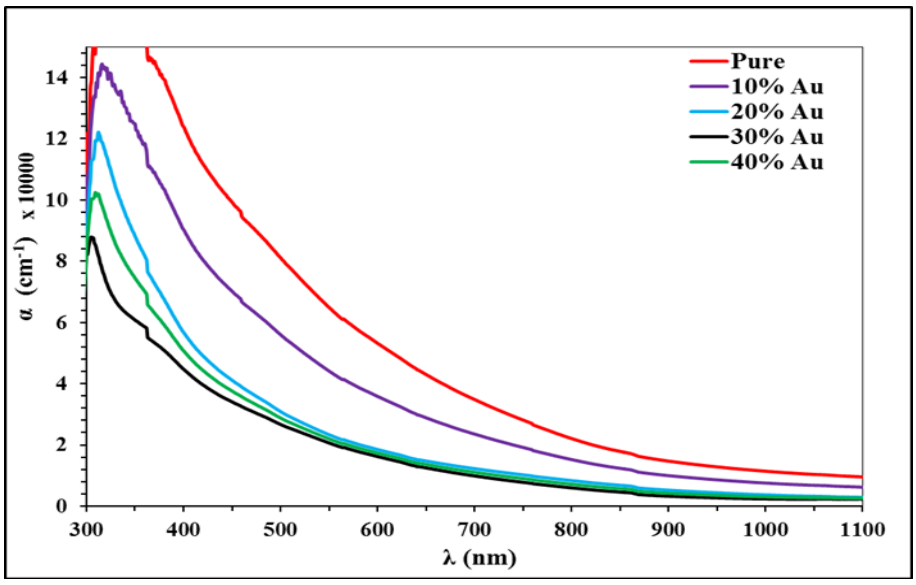

Fig.7: The absorption coefficient for pure WO_3 and doped of Au (0, 10, 20, 30 and 40)% as a function of wavelength.

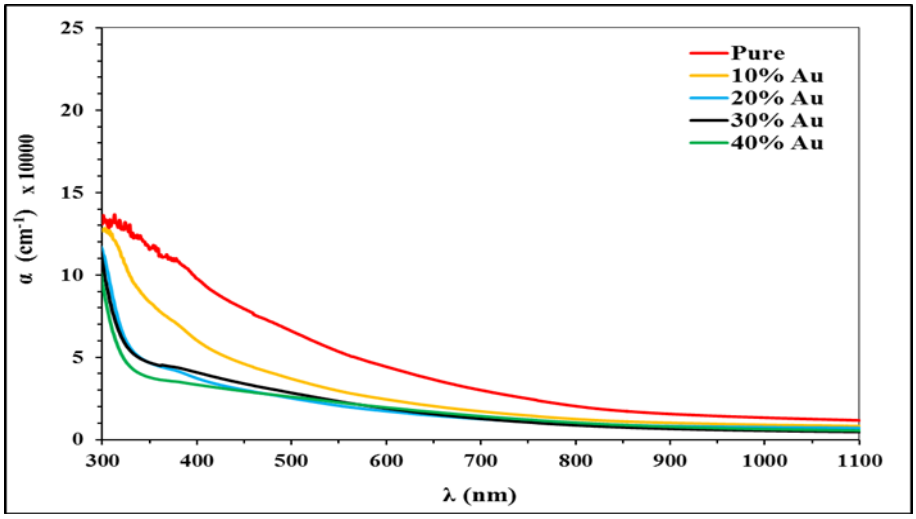

Fig.8: The absorption coefficient for pure WO_3 and doped of Au (0, 10, 20, 30 and 40)% as a function of wavelength at T_a=400 ˚C.

3-3 The optical energy gap

The values of the band gap of pure WO_3 thin film and doped with different concentration of gold nanoparticles can be determined by extrapolating the straight line portion of the $(\alpha h\nu)^2$ against $h\nu$, (see Fig. 9) at substrate temperature T_s= 250 ˚C, the results showed that the energy gap increases with increasing dopant ratio,

the increase in band gap from (2.80 eV) to (3.40 eV) is due to the effect of the dopant. Fig. 10 shows that the thin films at annealing temperature T_a = 400 °C it can be observed that (E_g) is increasing slightly with increasing of doping all films and changed from (2.65 eV) for pure film to (3.95 eV) for the ratio 40 % Au, (see Table 5) this results agree with Gullaplli and et al. [23], this is may be due to the effect of the dopant and annealing temperature.

The type of transition was directly allowed transition because the dependence of (α) on the photon energy (hv) was found to obey the following relationship [24]:

$$\alpha h\nu = B\,(h\nu - E_g)^r \qquad (5)$$

where E_g is the optical band gap, r the exponent depends upon the type of optical transitions in the material, hν is the energy of the incident photon, B the absorption edge width parameter.

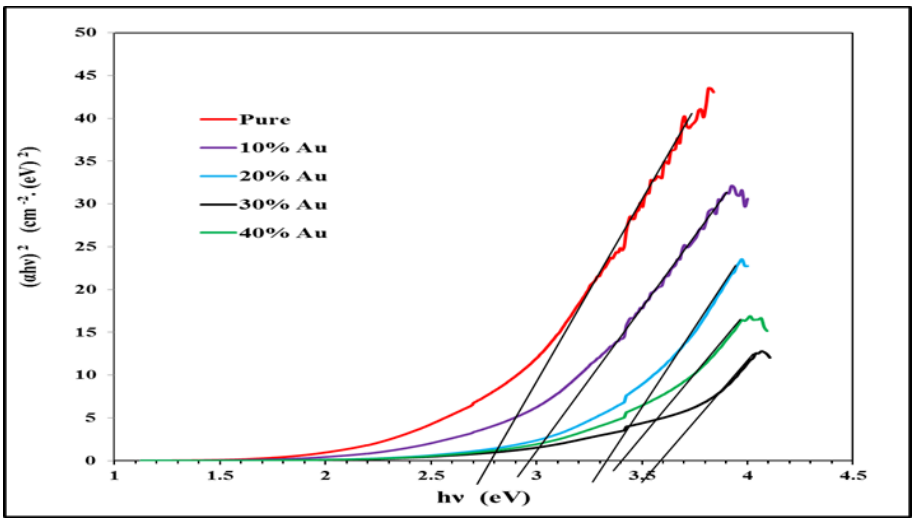

Fig. 9: The optical energy gap for pure WO_3 and doped of Au thin films.

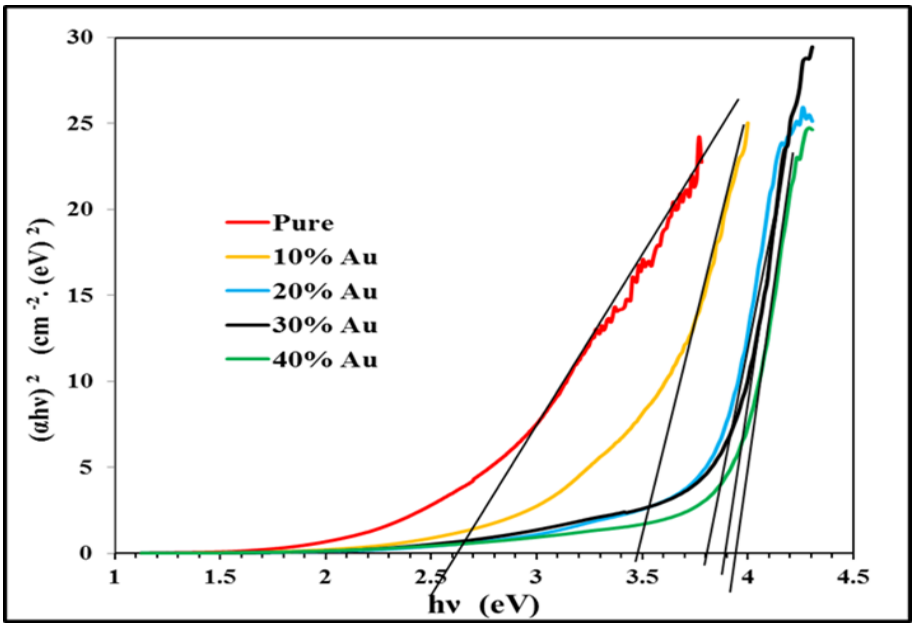

Fig. 10: The optical energy gap for pure WO_3 and doped of Au thin films with annealing temperature at T_a = 400 ˚C.

3-4 Extinction coefficient

Extinction coefficient (k) spectra versus wavelength in the range (300-1100 nm) as a function of different doping with Au is shown in Fig. 11 at T_s =250 ˚C, (see Table 4) it can be notes that (k) decreases at the absorption edge region this decrease is attributed to the decrease of the absorption coefficient due to the direct electronic transitions, it is clear from Fig. 12 that with the increase of Au concentration, and after annealing at 400 ˚C the extinction coefficient (k) decreases, it can be notes that (k) decrease at the absorption edge region(see Table 5), in general the extinction coefficient of annealing samples is smaller than that prepared before annealing. The Extinction coefficient (k) is calculated using the relation [25]:

$$k = \frac{\alpha\lambda}{4\pi} \quad (6)$$

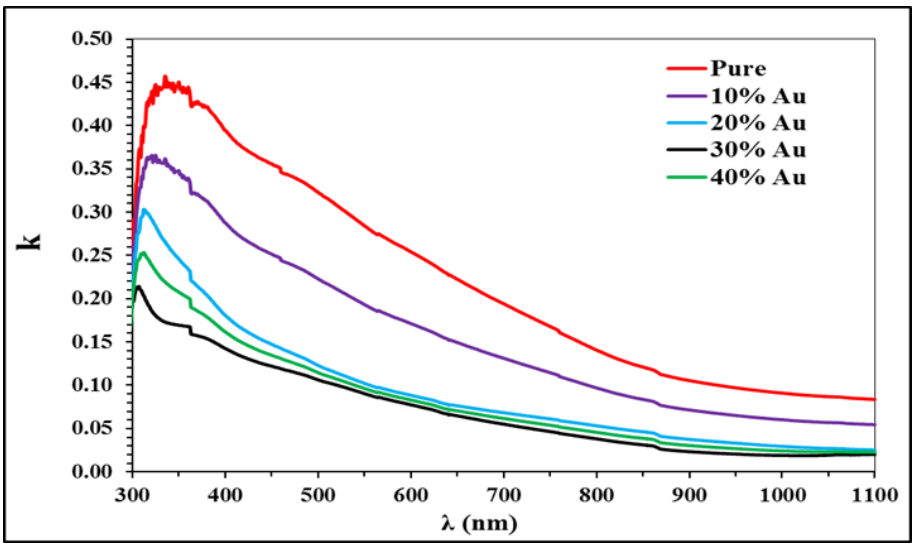

Fig. 11: The extinction coefficient for pure WO_3 and doped Au (0, 10, 20, 30 and 40)% thin films as a function of wavelength.

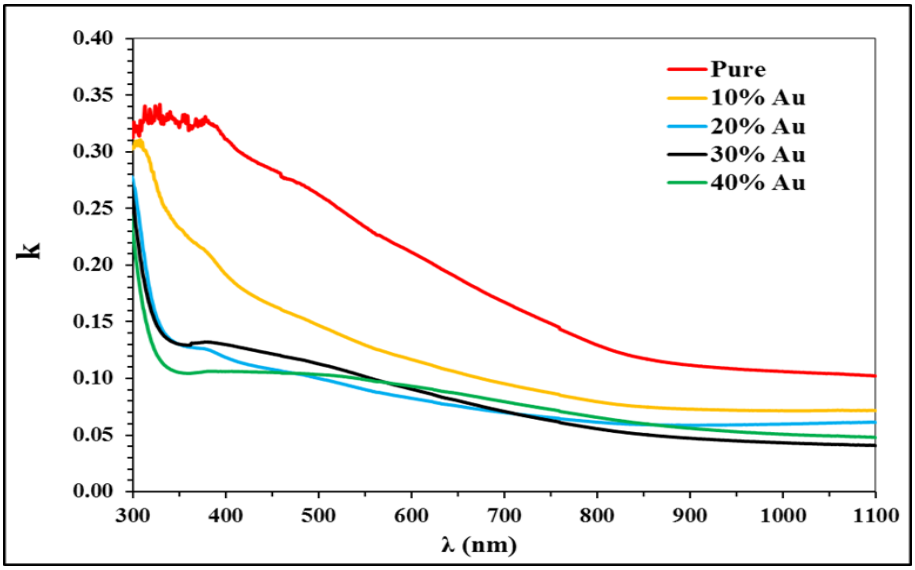

Fig. 12: The extinction coefficient for pure WO_3 and doped Au (0, 10, 20, 30 and 40)% thin films as a function of wavelength at T_a = 400 ˚C.

3-5 Refractive index

The variation of the refractive index as a function of the wavelength for pure WO_3 and doped Au thin films is illustrated in Figs. 13 and 14 at T_s= 250 ˚C and 400 ˚C annealing temperatures, it is clear from these figures that the refractive index increases with the increase in the wavelength of the incident photon, also it can be observed that the refractive index of the films increases with the increase in the doping ratio and annealing temperature (see Table 4 and 5), the increase in the refractive index may be correlated with the increase in the transmittance and the decrease in the absorption coefficient. The increase in the value of the refractive index with increasing wavelength shows normal dispersion behavior of the material [13]. The refractive index (n) is calculated using the relation [12]:

$$n = (1+ R^{1/2}) (1- R^{1/2}) \quad (7)$$

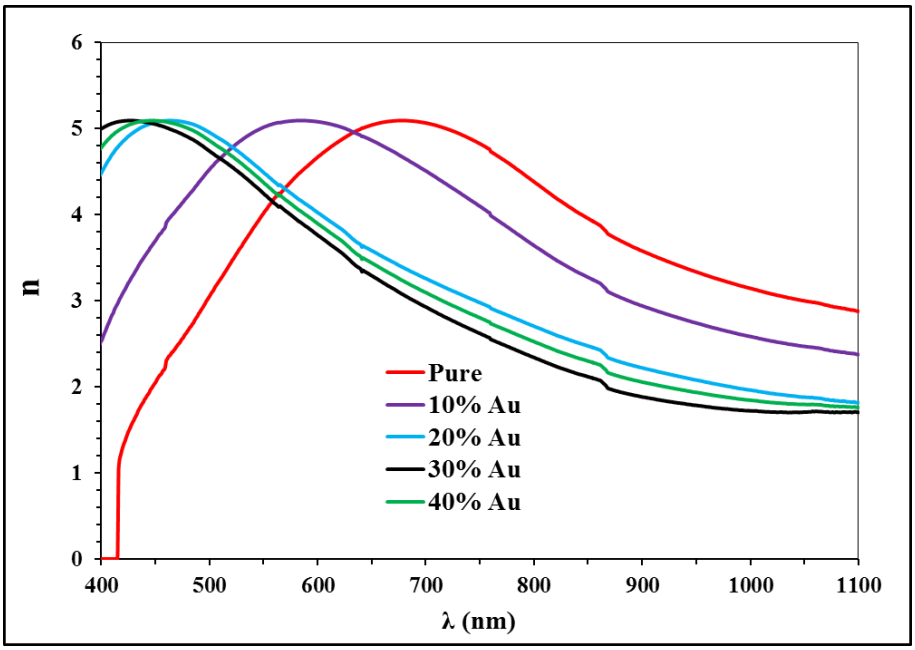

Fig. 13: Refractive index for pure WO_3 and doped of Au (0, 10, 20, 30 and 40) % thin films as a function of wavelength.

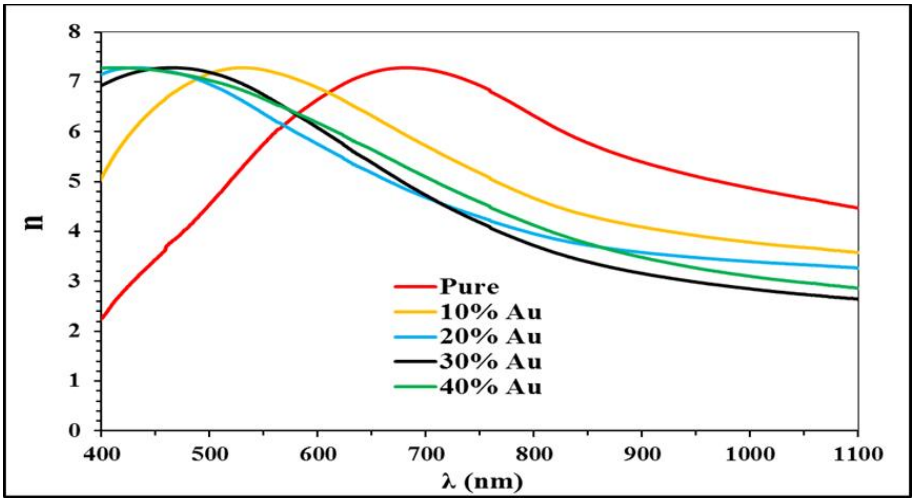

Fig. 14: Refractive index for pure WO_3 and doped of Au (0, 10, 20, 30 and 40) % thin films as a function of wavelength at T_a=400 ˚C.

3-6 The dielectric constant

Figs. 15-18 illustrate the variation of the real and imaginary part of the dielectric constant as a function of the wavelength for pure WO_3 and doped of Au with different ratios (0, 10, 20, 30 and 40)%, before and after annealing at 400 ˚C, the real part of the dielectric constant (ε_r) depends mainly on the value of (n^2), because of the smaller values of (k^2) comparison with (n^2), the imaginary part of the dielectric constant (ε_i) depends mainly on the (k) values which are related to the variations of the absorption coefficient (see Table 4 and 5). The real and imaginary parts of dielectric constant (εr, εi) respectively, were calculated by using these equations [12]:

$$\varepsilon_r = n^2 - k^2 \quad (8)$$

$$\varepsilon_i = 2nk \quad (9)$$

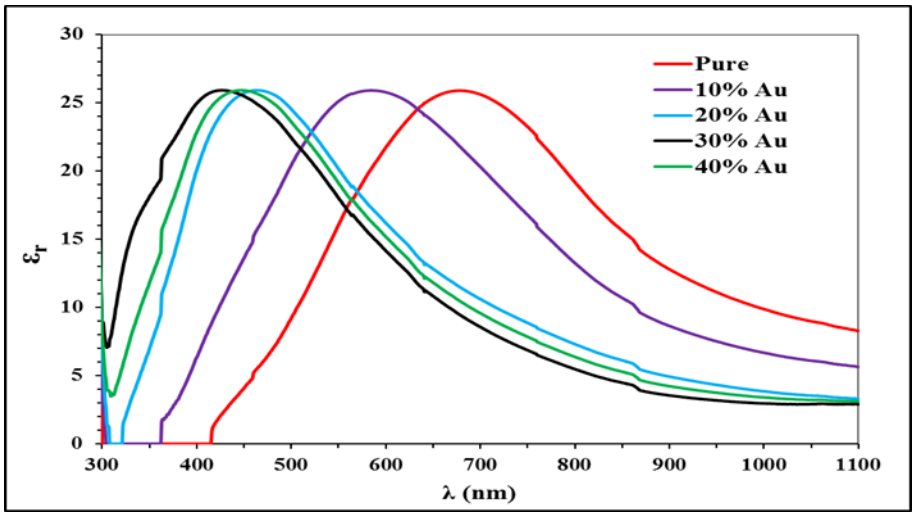

Fig. 15: The real part of dielectric constant for pure WO_3 and doped of Au (0, 10, 20, 30 and 40)% thin films as a function of wavelength.

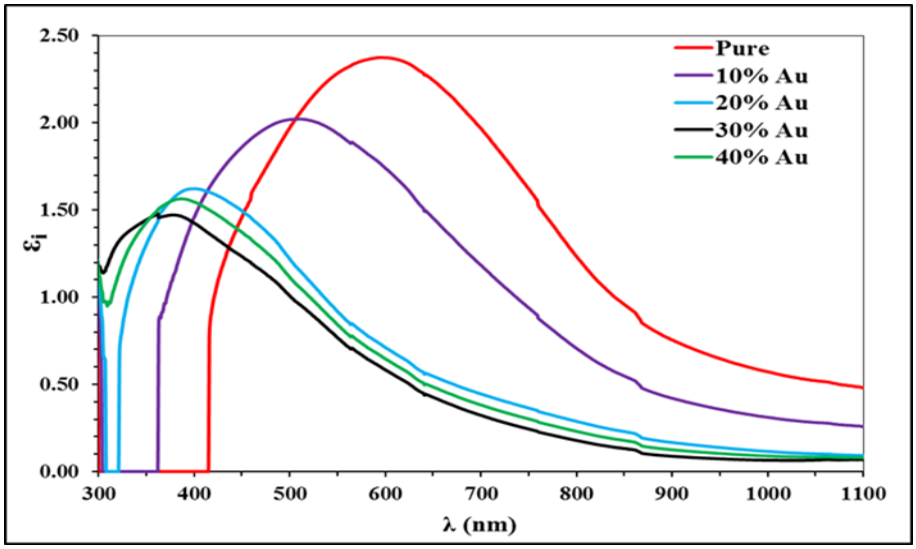

Fig. 16: The imaginary part of dielectric constant for pure WO3 and doped of Au (0, 10, 20, 30 and 40)% thin films as a function of wavelength.

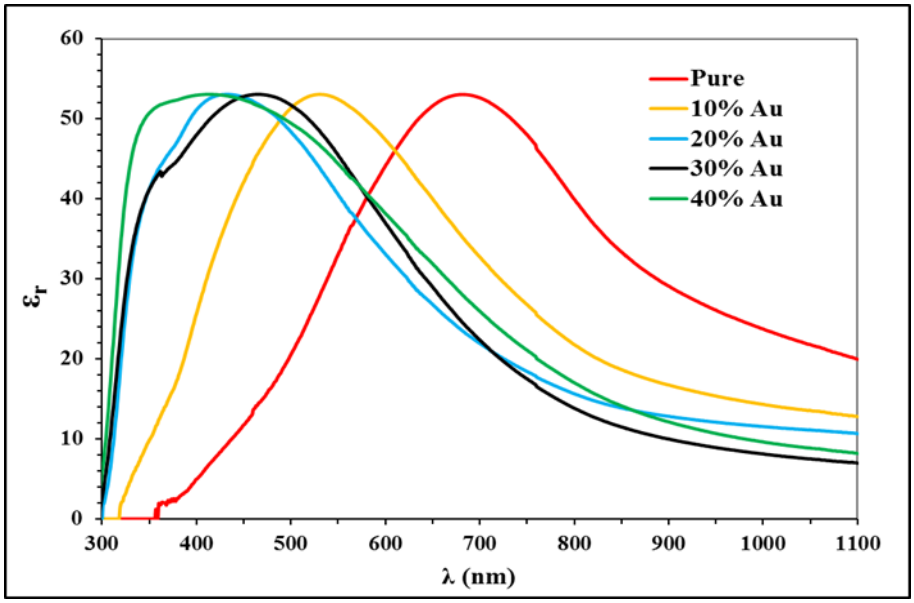

Fig. 17: The real part of dielectric constant for pure WO_3 and doped of Au (0, 10, 20, 30 and 40)% thin films as a function of wavelength at T_a= 400 ˚C.

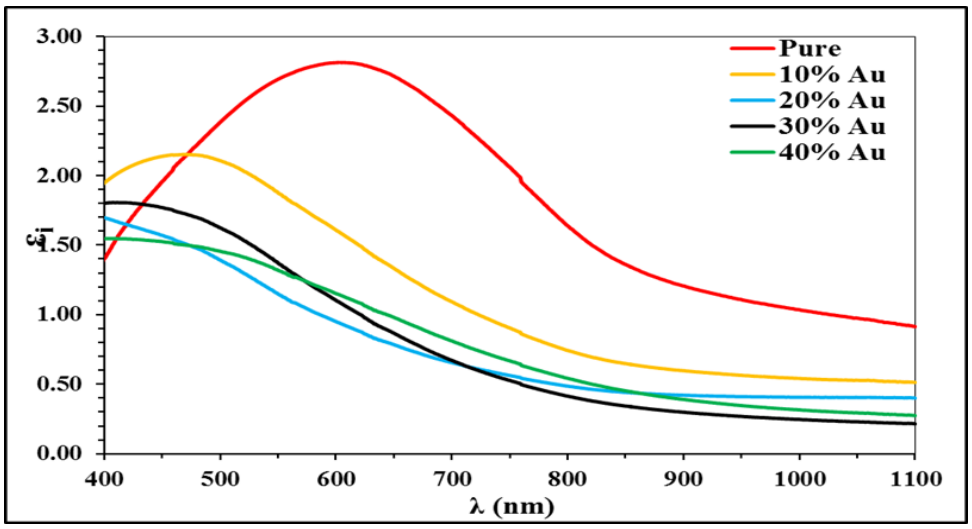

Fig. 18: The imaginary part of dielectric constant for pure WO_3 and doped of Au (0, 10, 20, 30 and 40) % thin films as a function of wavelength at T_a= 400 ˚C.

Table 4: The optical energy gap and the optical constants parameters for pure WO_3 and different doping of Au thin films at λ = 500 nm.

Au %	T%	α (cm^{-1})	K	n	ε_r	ε_i	E_g(ev)
0	3.89	81169	0.323	3.050	9.198	1.971	2.80
10	10.63	56041	0.223	4.525	20.424	2.019	3.00
20	29.04	30912	0.123	4.956	24.544	1.220	3.30
30	34.34	26721	0.106	4.740	22.456	1.008	3.60
40	31.58	28816	0.115	4.861	23.614	1.115	3.40

Table 5: The optical energy gap and the optical constants parameters for pure WO_3 and different doping of Au thin films at T_a = 400 ˚C at λ = 500 nm.

Au%	T%	α (cm^{-1})	K	n	ε_r	ε_i	E_g(ev)
0	1.92	65904	0.262	4.542	20.563	2.383	2.65
10	10.91	36932	0.147	7.167	51.351	2.108	3.50
20	22.09	25164	0.100	6.958	48.404	1.394	3.80
30	18.22	28381	0.113	7.193	51.726	1.625	3.95
40	21.00	26012	0.104	7.035	49.476	1.457	3.90

Conclusions

The WO_3 thin film with different doping concentration of Au nanoparticles (0, 10, 20, 30 and 40)% wt. based on chemical spray pyrolysis deposition have been prepared on glass substrate at T_s =250 ˚C successfully. The X-ray diffraction pattern of WO_3:Au at substrate temperature 250 ˚C show amorphous, but with annealing temperature the structure will became a polycrystalline for different doping concentration of gold nanoparticles. The absorption coefficient in general with the increasing of doping ratio decreases for all samples, and have value ($\alpha > 10^4$ cm^{-1}), the refractive index and extinction coefficient and dielectric constant (real and imaginary parts) in general, are increase with the increasing of doping ratio for all samples before and after annealing.

References

[1] Fumiaki Mitsugi, Eiichi Hiraiwa, Tomoaki Ikegami, Kenji Ebihara, Raj Kumar Thareja Japanese, Journal of Applied Physics, 41 (2002) 5372-5375.

[2] S. K. Gullapalli, R. S. Vemuri, C. V. Ramana, Applied Physics Letters, 96 (2010) 1-3.

[3] K.J. Patel, CJ. Panchal, VA. Kheraj, MS Desai Materials Chemistry and Science, 114, Issue 1 (2009) 475-478.

[4] Maosong Tong, Guorui Dai, Yuanda Wu, Xiuli He, Dingsan, Journal of Materials Science, 36 (2001) 2535-2538.

[5] G. Slewah, M.Sc. Thesis, Enhancement the performance of liquid crystal switch by doping CdS quantum dot., College of Sciences, University of Basrah, (1990).

[6] P. Sen, J. Ghosh, A. Abdullah, P. Kumar, Vandana Indian Acad. Sci. (Chem. Sci.), (2003), 499-508. Proc.

[7] A. R. Siekkinen, J. M. McLellan, J. Chen, Y. Xia, Chemical Physics Letters (2006) 432- 491.

[8] Liz-Marzán LM, Langmuir, 22 (2006) 32-41.

[9] R. Shukla, V. Bansal, M. Chaudhary, A. Basu, R. R. Bhonde, M. Sastry, Langmuir, 21 (2005) 10644-10654.

[10] M. C. Daniel, D. Astruc, Chem. ReV., 104 (2004) 293-346.

[11] Lai, Wei Hao, Materials Transactions, 48.6 (2007) 1575-1577.

[12] Dong-myong, Molecular Diversity Preservation International, 12, 5 (2005) 519-528.

[13] A.A. Akl, S.A. Aly, Journal of Material Sciences (2016) 2321-6212.

[14] Ganbavle, Journal of Materials Engineering and Performance, 23 (2014) 1204-1213.

[15] H. Rezvani, Indian Journal of Science, 3, 6 (2010) 0974-6846.
[16] Lijun Li, Ke Yu, Zheng Tang, Ziqiang Zhu, Qing Wan, Journal of Applied Physics, 107 (2010) 107-134.
[17] Jae Cheon Sohn, Sung Eun Kim, Zee Won Kim, Yu, Transactions on Electrical and Electronic Materials, 10, 4 (2009) 614-714.
[18] Joseph, V. Mathew, K.E Ibraham, Chinese Journal of Physics, 45, 1 (2007) 84-97.
[19] Y. Sitrotin and M. Shaskolskaya, "Fundamental of crystal physics", Mir publishers, Moscow, (1982).
[20] J. A. Wingrave and C. R. C.Press., "Oxide surfaces", Marcel Dekker, New York, 2001.
[21] P. Tyagi and A. G. Vedeshwar, Phys. Rev. B 66, 075422 (2002) 7-15.
[22] F. Z. Tepehan, F. E. Ghodsi, N. Ozer, G. G. Tepehan, Sol. Energy Mater. Sol. Cells, 59 (1999) 265-275.
[23] SK. Gullapalli, RS. Vemuri, Ramana, Applied Physics Letters, 17, 96(2010) 108-112.
[24] M.G. Hutchins, O. Abu-Alkhair, M.M. El-Nahass, K. Abd El-Hady, Mater. Chem. Phys., 98, 401 (2006) 2-3.
[25] M. Thakurdesai, N. Kukarni, B. Chalke, A. Mahadkar, Calcogenide Letters, 8, 3 (2011) 223-229.